EARTH PRESSURES ON RETAINING WALLS DUE TO ANISOTROPIC AND NONHOMOGENEOUS BACKFILLS

A. SIVA REDDY AND R. J. SRINIVASAN*

(Department of Civil Engineering, Indian Institute of Science, Bangalore)

Received on February 28, 1976 and in revised form on June 22, 1976

ABSTRACT

In this paper an attempt is made to study the lateral earth pressures on retaining walls as affected by anisotropy and non-homogeneity with respect to cohesion, of the backfill. Both the passive and active conditions are studied and the method of characteristics is used in the analysis. Numerical results show that, as the coefficient of anisotropy, k, *defined as the ratio of vertical strength to horizontal strength, changes from* 0·8 *to* 2, *the pressure at the top of the wall decreases considerably. Also, as* k *changes from* 0·8 *to* 2, *the modified passive and active earth pressure coefficients decrease when cohesion increases with depth and are unaffected by* k *when cohesion is constant with depth. On the other hand, when the rate of increase of cohesion with depth increases, the modified earth pressure coefficients are found to increase considerably.*

Key words: Anisotropy, Earth Pressure, Homogeneity, Plastic Equilibrium, Retaining Walls, Soil Mechanics.

INTRODUCTION

The study of lateral earth pressures is important in the design of retaining walls and timbering of cuts, in the calculation of bearing capacity of foundations and of pressures in soils, and in several other problems. The use of the method of characteristics for solution of the problem has received much attention in recent years, principally due to the work of Sokolovsky [1] who presented a numerical integration procedure for the calculation of active and passive earth pressures on retaining walls due to soils having both cohesion and internal friction. Using Sokolovsky's approach, Wack [2] and Hajal [3] presented passive earth pressure coefficients for walls having horizontal and inclined back fill surfaces, respectively. Natural

* Present Address: Department of Transportation Technology, University of Technology, Loughborough, England.

soil deposits exhibit anisotropy and non-homogeneity in shear strength to a certain degree. In this paper, the influence of anisotropy and non-homogeneity on the resultant pressure at the top of the wall as well as on the earth pressure coefficients, is studied.

ASSUMPTIONS

At any point in the soil mass behind the retaining wall, the variation of cohesion with direction is expressed by the following equation [4] which was originally proposed by Casagrande and Carrillo [5].

$$c = c_H + (c_V - c_H) \sin^2 \psi \tag{1}$$

in which, c = cohesion on planes corresponding to any value of ψ; $\psi = \theta_i - 45° + \phi/2$; θ_i = inclination of a slip line of the $(\psi + \mu)$—family to the x-axis (Fig. 1); ϕ = angle of internal friction; $\mu = 45° - \phi/2$; and c_H, c_V = cohesion along planes corresponding to ψ equal to 0° and 90°, respectively.

Since ψ is defined as above it has been shown by Shaklarsky and Livnch [6] that there are two conjutate failure planes at the point considered (Fig. 1).

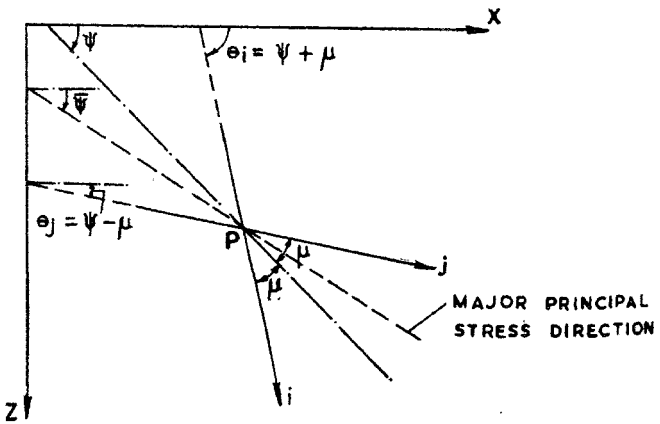

FIG. 1. Orientations of slip lines.

In addition to the above assumption of anisotropy, it is assumed that the cohesion in a given direction increases linearly with depth, as expressed by

$$c_v = c_{vs} + \alpha Z \tag{2}$$

in which,

c_{vs} = the value of c_v at the ground surface,

α = rate of variation of c_v with depth, and

z = depth below ground surface.

The ratio c_v/c_H at any point, is designated as the coefficient of anisotropy, k, and this is assumed to be constant throughout the soil mass.

In order to express all quantities in terms of non-dimensional variables, the stresses are divided by c_{vs}, which is a characteristic stress, and the distances are divided by the characteristic length, $l = c_{vs}/\gamma$, wherein γ is the unit weight of the soil

Equation (1) is therefore written as

$$c = c_v\left[\frac{1 + (k-1)\sin^2\psi}{k}\right]. \tag{3}$$

Dividing equation (3) by c_{vs} and with the notation that all quantities with primes are dimensionless quantities,

$$c' = \frac{c_v}{c_{vs}}\left[\frac{1 + (k-1)\sin^2\psi}{k}\right].$$

Dividing equation (2) by c_{vs} and also introducing the dimensionless quantity z' gives

$$c_v' = 1 + \frac{\alpha l z'}{c_{vs}} = 1 + \beta_c z' \tag{4}$$

in which $\beta_c = \alpha l/c_{vs}$ = dimensionless parameter representing the increase of cohesion with depth.

Analysis for Passive Earth Pressure

The line OL (Fig. 2 *a*) represents the retaining wall having an angle of wall friction, δ, whose value ranges from 0 to ϕ. In order to determine the earth pressure acting along the wall, first the state of stress at any point

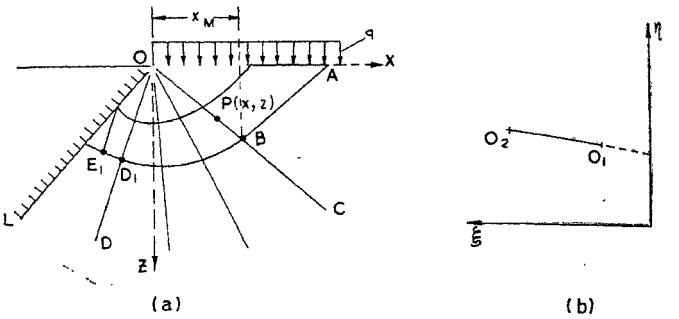

FIG. 2. Calculation of points along the wall.

in the soil mass which is in plastic equilibrium, is considered and the following expressions are obtained for the normal stresses σ_x, σ_z and tangential stress τ_{xz} (Shaklarsky and Livneh [6] and Siva Reddy and Srinivasan [7])

$$\sigma_x = \sigma(1 + \sin\phi \cos 2\psi) - H - \frac{1}{2}\frac{\partial c}{\partial \psi}\cos\phi \sin 2\psi \tag{5}$$

$$\sigma_z = \sigma(1 - \sin\phi \cos 2\psi) - H + \frac{1}{2}\frac{\partial c}{\partial \psi}\cos\phi \sin 2\psi \tag{6}$$

$$\tau_{xz} = \sigma \sin\phi \sin 2\psi + \frac{1}{2}\frac{\partial c}{\partial \psi}\cos\phi \cos 2\psi \tag{7}$$

in which,

$$\sigma = \frac{\sigma_x + \sigma_z}{2} + H, \tag{8}$$

and

$$H = c \cot\phi. \tag{9}$$

The above equations which express the stresses σ_x, σ_z and τ_{xz} in terms of only two variables, σ and ψ, are then substituted into the equilibrium equations

$$\frac{\partial \sigma_x}{\partial x} + \frac{\partial \tau_{xz}}{\partial z} = 0 \tag{10}$$

$$\frac{\partial \sigma_z}{\partial z} + \frac{\partial \tau_{xz}}{\partial x} = \gamma. \tag{11}$$

On manipulation of the resulting equations in the same way as done by Sokolovsky [1] and using the following dimensionless variables:

$$\xi = \frac{\cot\phi}{2} \log_e \sigma^* + \psi \tag{12}$$

$$\eta = \frac{\cot\phi}{2} \log_e \sigma^* - \psi \tag{13}$$

wherein, $\sigma^* = \sigma/c_{vs}$, the following relationships are obtained along the two families of characteristics or slip lines:

Along the $(\psi + \mu)$-family:

$$\frac{dz'}{dx'} = \tan(\psi + \mu) \tag{14}$$

$$\frac{d\xi}{dx'} + A_1 \frac{d\psi}{dx'} = A_3, \tag{15}$$

and along the $(\psi - \mu)$-family:

$$\frac{dz'}{dx'} = \tan(\psi - \mu) \tag{16}$$

$$\frac{d\eta}{dx'} + A_2 \frac{d\psi}{dx'} = A_4 \tag{17}$$

in which,

$$A_1 = \frac{-\cot\phi}{2\sigma^*}\left[\frac{1}{c_{vs}} \cot\phi \frac{\partial c}{\partial \psi} - \frac{1}{2}\frac{\partial^2 c}{\partial \psi^2}\right], \tag{18}$$

$$A_2 = -\frac{\cot\phi}{2\sigma^*}\frac{1}{c_{vs}}\left[\cot\phi \frac{\partial c}{\partial \psi} + \frac{1}{2}\frac{\partial^2 c}{\partial \psi^2}\right], \tag{19}$$

$$A_3 = \frac{\gamma l}{c_{vs}} \frac{\cos(\psi - \mu)}{2\sigma^* \sin\phi \cos(\psi + \mu)} + \frac{\cot\phi}{2\sigma^*}\left[f_2 \beta_c \frac{\gamma l}{c_{vs}} \frac{\cos(\psi - \mu)}{\sin\phi \cos(\psi + \mu)} - \frac{f}{2}\beta_c \tan(\psi + \mu)\right], \tag{20}$$

$$A_4 = \frac{-\gamma l}{c_{vs}} \frac{\cos(\psi + \mu)}{2\sigma^* \sin\phi \cos(\psi - \mu)} + \frac{\cot\phi}{2\sigma^*} \times \left[\frac{-f_2 \beta_c \frac{\gamma l}{c_{vs}} \cos(\psi + \mu)}{\sin\phi \cos(\psi - \mu)} + \frac{f}{2}\beta_c \tan(\psi - \mu)\right] \tag{21}$$

$$f = \frac{k-1}{k} \sin 2\psi,$$

and

$$f_2 = \frac{1 + (k-1)\sin^2 \psi}{k}.$$

Equations (14) through (17) may be used to determine x', z', ξ and η at the points of intersection of the characteristics as explained below (Sokolovsky [1]):

Figure 3 shows a slip line of the $(\psi + \mu)$-family passing through point B and a slip line of the $(\mu - \psi)$-family passing through point A. The two slip lines intersect at a point C at which x', z', ξ, η, σ^* and ψ are to be determined, the values at points A and B being known completely.

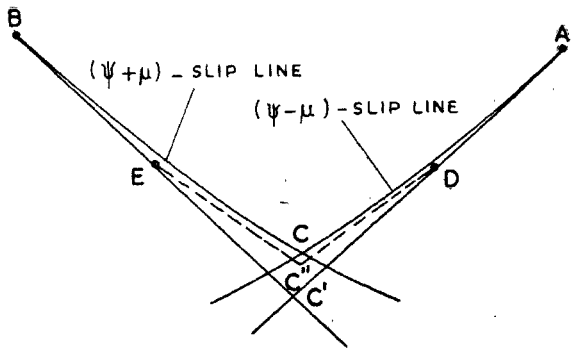

FIG. 3. Calculation of a new point in the passive case.

Using subscript A for the quantities at A and subscript B for the quantities at B, equations (14) through (17) may be written in finite difference form and solving these the following equations are obtained:

$$x' = \frac{x'_A \tan(\psi_A - \mu) - z'_A - x'_B \tan(\psi_B + \mu) + z'_B}{\tan(\psi_A - \mu) - \tan(\psi_B + \mu)} \tag{22}$$

$$z' = z'_B + (x' - x'_B)\tan(\psi_B + \mu) \tag{23}$$

$$\psi = \frac{1}{(A_1 - A_2 + A_2)} [\xi_B + A_1\psi_B + A_3 (x' - x'_B) - \eta_A - A_2\psi_A - A_4 (x' - x'_A)] \quad (24)$$

$$\xi = \xi_B + A_1 (\psi_B - \psi) + A_3 (x' - x'_B) \quad (25)$$

$$\eta = \eta_A + A_2 (\psi_A - \psi) + A_4 (x' - x'_A). \quad (26)$$

By using the above equations, with A_1, A_2, A_3, A_4 and ψ being those corresponding to the points A or B, a point C' (Fig. 3) is obtained. However, the required point is C and in order to obtain this point more accurately, the calculations are repeated by treating the mid points D and E of the lines AC' and BC' as the known points and using the values of σ^* and ψ at C' incalculating the coefficients A_1 to A_4 and using ψ at C' in place of ψ_A and ψ_B in the above equations (Wack [2]). Thus the point C'' is obtained and this is assumed to represent the point C itself.

Analysis when $\phi = 0$

In this case, in place of σ, the variable p is used wherein,

$$p = \frac{\sigma_x + \sigma_z}{2}.$$

The following expressions are obtained for the stresses σ_x, σ_z and τ_{xz}, by following the same procedure as in case of soils with internal friction (Siva Reddy and Srinivasan [7]):

$$\sigma_x = p - \frac{1}{2}\frac{\partial c}{\partial \psi} \sin 2\psi + c \cos 2\psi \quad (27)$$

$$\sigma_z = p + \frac{1}{2}\frac{\partial c}{\partial \psi} \sin 2\psi - c \cos 2\psi \quad (28)$$

$$\tau_{xz} = \frac{1}{2}\frac{\partial c}{\partial \psi} \cos 2\psi + c \sin 2\psi. \quad (29)$$

From equations (27) through (29), σ_x, σ_z and τ_{xz} are substituted into equations (10) and (11). On manipulation of these equations in the same way as in the previous case and using the dimensionless variables:

$$\xi = \frac{p'}{2} + \psi \quad (30)$$

$$\eta = \frac{p'}{2} - \psi \quad (31)$$

wherein, $p' = p/c_{vs}$, the following relationships are obtained along the two families of slip lines:

Along the $(\psi + \mu)$-family:

$$\frac{dz'}{dx'} = \tan\left(\psi + \frac{\pi}{4}\right) \tag{32}$$

$$\frac{d\xi}{dx'} + E_1 \frac{d\psi}{dx'} = E_2 \tag{33}$$

and along the $(\psi - \mu)$-family:

$$\frac{dz'}{dx'} = \tan\left(\psi - \frac{\pi}{4}\right) \tag{34}$$

$$\frac{d\eta}{dx'} - E_1 \frac{d\psi}{dx'} = E_3 \tag{35}$$

in which,

$$E_1 = \frac{1}{2}(1 + \beta_c z')\left(\frac{f_1}{2} + 2f_2\right) - 1 \tag{36}$$

$$E_2 = \frac{1}{2}\left[\left(1 - \frac{f\beta_c}{2}\right)\tan\left(\psi + \frac{\pi}{4}\right) - f_2\beta_c\right] \tag{37}$$

$$E_3 = \frac{1}{2}\left[\left(1 + \frac{f\beta_c}{2}\right)\tan\left(\psi - \frac{\pi}{4}\right) - f_2\beta_c\right] \tag{38}$$

and

$$f_1 = \frac{k-1}{k} 2\cos 2\psi.$$

The following expressions are obtained by writing equations (32) through (35) in finite difference form:

$$x' = \frac{x'_A \tan\left(\psi_A - \frac{\pi}{4}\right) - z'_A - x'_B \tan\left(\psi_B + \frac{\pi}{4}\right) + z'_B}{\tan\left(\psi_A - \frac{\pi}{4}\right) - \tan\left(\psi_B + \frac{\pi}{4}\right)} \tag{39}$$

$$z' = z'_B + (x' - x'_B)\tan\left(\psi_B + \frac{\pi}{4}\right) \tag{40}$$

$$\psi = \frac{1}{2E_1 + 2}\left[\xi_B + E_1\psi_B + E_2(x' - x'_B) - \eta_A + E_1\psi_A - E_3(x' - x'_A)\right] \quad (41)$$

$$\xi = \xi_B + E_1(\psi_B - \psi) + E_2(x' - x'_B) \quad (42)$$

$$\eta = \eta_A - E_1(\psi_A - \psi) + E_3(x' - x'_A). \quad (43)$$

Expressions for the Stresses Along the Boundary of the Rankine Zone

The following expression is obtained for o^* along the line OB, the boundary of the Rankine zone (Fig. 2 *a*) :

$$o^* = \frac{\frac{\gamma 1}{c_{\gamma s}}z' + p}{1 - \sin\phi} + \frac{\beta_c z' \cot\phi}{k(1 - \sin\phi)} \quad (44)$$

in which,

$$p = \frac{q}{c_{\gamma s}} + \frac{\cot\phi}{k}. \quad (45)$$

For ϕ equal to zero, the expression for p' along the boundary OB is

$$p' = \frac{\gamma 1}{c_{\gamma s}}z' + p + \frac{1}{k}(1 + \beta_c z'). \quad (46)$$

Determination of Points Along OL

The change of η at the point O along O_1O_2 (Fig. 2 *b*) is obtained from equation (17) as

$$\triangle\eta = -A_2\triangle\psi. \quad (47)$$

From equation (47) the change in η at O can be found by knowing ψ at O_2. By transformation from x, z coordinates to n, t coordinates the following expressions are obtained for the stresses σ_n and τ_{nt} along OL:

$$\sigma_n = \sigma[1 + \sin\phi\cos 2(\psi - \theta_0)] - H - \frac{1}{2}\frac{\partial c}{\partial\psi}\cos\phi\sin 2(\psi - \theta_0) \quad (48)$$

$$\tau_{nt} = -\sigma\sin\phi\sin 2(\psi - \theta_0) - \frac{1}{2}\frac{\partial c}{\partial\psi}\cos\phi\cos 2(\psi - \theta_0). \quad (49)$$

The following relationship holds along the line OL

$$\tau_{nt} = -(\sigma_n + H)\tan\delta \quad (50)$$

in which the maximum value that δ can take is ϕ, corresponding to the critical condition in this case. In retaining walls δ is the angle of wall friction.

Substituting for σ_n and τ_{nt} from equations (48) and (49) into equation (50) and simplifying yields the following relationship:

$$\sin(2\psi - 2\theta_0 - \delta) = \frac{\sin\delta}{\sin\phi} - \frac{\cot\phi}{2\sigma^*}\frac{\partial c}{\partial\psi}\cos(2\psi - 2\theta_0 - \delta). \tag{51}$$

The expression for σ^* to be substituted in equaion (51) is obtained as follows:

If η_1 and ψ_1 refer to the point E_1 on the characteristic OD (Fig. 2 *a*), then from equations (17) and (13) the following expression for σ^* is obtained:

$$\sigma^* = \exp\left\{\frac{2}{\cot\phi}\left[\eta_1 + (1 - A_2)\psi + A_2\psi_1 + A_4(x' - x_1')\right]\right\}. \tag{52}$$

Using equation (16)

$$x' = \frac{z_1' - x_1'\tan(\psi_1 - \mu)}{m - \tan(\psi_1 - \mu)} \tag{53}$$

in which, m = slope of the line $OL = -\tan(90 - \theta_0)$.

Substitution for σ^* from equation (52) into equation (51) leads to a transcendental equation in ψ which may be solved by an iteration procedure to obtain ψ. Substitution of this ψ back into equation (52) gives σ^* and from these values, ξ and η may be found.

Computation of Points Along OL in the Case $\phi = 0$

In this case the condition to be satisfied along the line OL is

$$\tau_{nt} = -c. \tag{54}$$

The following are the expressions obtained for the stresses σ_n and τ_{nt} along OL:

$$\sigma_n = p + c\cos 2(\psi - \theta_0) - \frac{1}{2}\frac{\partial c}{\partial\psi}\sin 2(\psi - \theta_0) \tag{55}$$

$$\tau_{nt} = -c\sin 2(\psi - \theta_0) - \frac{1}{2}\frac{\partial c}{\partial\psi}\cos 2(\psi - \theta_0). \tag{56}$$

Substituting for τ_{nt} in equation (54) and simplifying leads to the following equation

$$1 + (k-1)\sin^2\psi - \left(1 + \frac{k-1}{2}\right)\sin 2(\psi - \theta_0) - \frac{k-1}{2}\sin 2\theta_0 = 0 \tag{57}$$

From the above equation it is seen that ψ is dependent on k and θ_0 only. Hence, for given k and θ_0, ψ is constant along OL. The calculation of a point along OL which is the intersection of a characteristic of the $(\psi - \mu)$-family with the non-characteristic OL, is done in the same manner as in the previous case after knowing ψ from solution of equation (57). The equivalent normal pressure $(\sigma_n + H)$ is determined from equation (48) for several points along the wall, OL. The resultant pressure at any point on OL is

$$P_p = \frac{\sigma_n + H}{\cos\delta},$$

and the dimensionless resultant pressure, P_p' is given by

$$P_p' = \frac{P_p}{c_{vs}}. \tag{58}$$

The relationship between P_p' and the distance L, along the wall is asymptotic to a straight line as L increases and does not deviate much from this straight line at smaller values of L. Hence the toal force acting on the wall can be calculated from the resultant pressure at the top of the wall and the slope of the straight line asymptote.

Analysis for Active Earth Pressure

Figure 4 shows the zones of plastic failure behind a retaining wall in the active case for an isotropic and homogeneous backfill (Sokolovsky, [1]). In the case of the anisotropic and non-homogeneous medium considered herein, the state of stress at any point is given by equations (5) through (7). Hence, the relationships along the two families of slip lines are the same as in equations (14) through (17). However, the relative positions of the two families of slip lines are interchanged in this case (Fig. 4) when compared to the passive case. Therefore, for calculation of points of intersection of the characteristics, equations (22) through (26) are used. The points A and B are on the $(\psi - \mu)$ and $(\psi + \mu)$-slip lines respectively (Fig. 5).

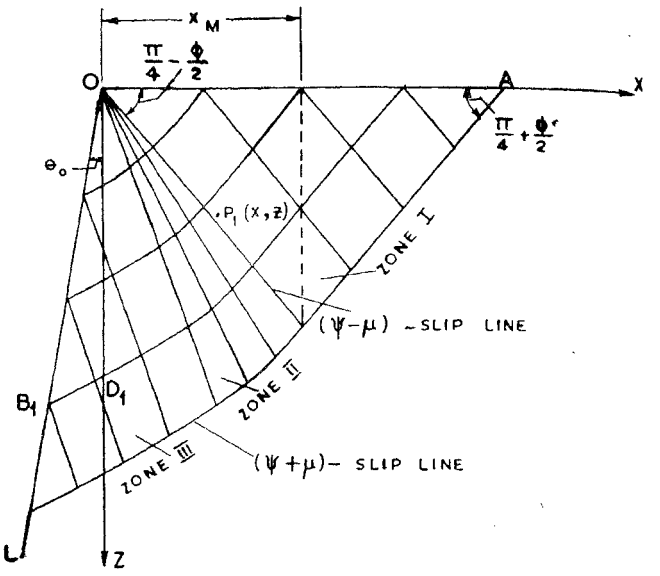

FIG. 4. Zones of plastic failure behind a wall in the active case

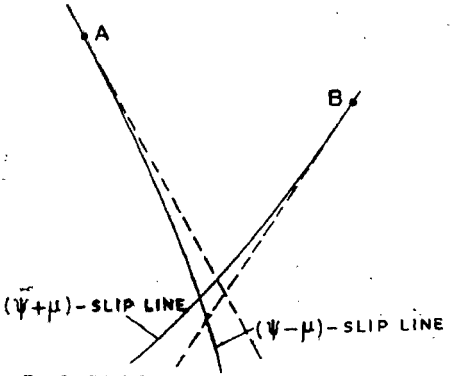

FIG. 5. Calculation of a new point in the active case.

The point O is a limiting slip line of the $(\psi + \mu)$-family along which equation (15) holds. Writing this equation in finite difference form, gives the change in ξ along O_1O_2 as

$$\triangle \xi = - A_1 \triangle \psi \tag{59}$$

in which,

$$A_1 = \frac{- \cot \phi}{2\sigma^*} \frac{1}{c_{vs}} \left(\cot \phi \frac{\partial c}{\partial \psi} - \frac{1}{2} \frac{\partial^2 c}{\partial^2 \psi} \right) \triangle \psi. \tag{60}$$

In order to find the quantities, σ^* and ψ at point O, these are first determined for the point O_2 (Fig. 2 *b*) as explained below, by using equation (50).

The expression for σ_n in this case is same as that in the passive case, and τ_{nt} is given by

$$\tau_{nt} = \sigma \sin \phi \sin 2 (\psi - \theta_0) + \frac{1}{2} \frac{\partial c}{\partial \psi} \cos \phi \cos 2 (\psi - \theta_0) \tag{61}$$

Substitution for σ_n and τ_{nt} from equations (48) and (61) into equation (50) and simplification, yields the following condition along the wall:

$$\sin (2\psi - 2\theta_0 + \delta) = - \frac{\sin \delta}{\sin \phi} - \frac{\cot \phi}{2\sigma^*} \frac{1}{c_{vs}} \frac{\partial c}{\partial \psi} \cos (2\psi - 2\theta_0 + \delta). \tag{62}$$

The value of ψ along the wall is determined by solving equation (62). In the case of isotropic medium, $\partial c/\partial \psi$ in equation (62) is zero and ψ is obtained explicitly as

$$\psi = \frac{\pi}{2} + \frac{\triangle}{2} + \theta_0 - \frac{\delta}{2} \tag{63}$$

in which

$$\triangle = \sin^{-1} \left(\frac{\sin \delta}{\sin \phi} \right). \tag{64}$$

Equation (63) is same as that derived by Sokolovsky [1].

If ξ_1 is the value of ξ at a point previous to the point O_2, along O_1O_2 (Fig. 2 *b*) then equation (59) may be written as

$$\xi - \xi_1 + A_1 \triangle \psi = 0. \tag{65}$$

Substitution for ξ from equation (12) and solving for σ^* gives the following relationship:

$$\sigma^* = \exp \frac{2}{\cot \phi} (\xi_1 - A_1 \triangle\psi - \psi) \tag{66}$$

ψ is determined from equations (62) and (66) by iteration.

If D_1 is the last point on a $(\psi - \mu)$-family slip line, before the point B_1 on the wall (Fig. 4) and the quantities at point D_1 are denoted as x_1', z_1', ξ_1, σ_1^* and ψ_1, then using equations (14) and (15), the equations along D_1B_1 are written as

$$z' - z_1' = (x' - x_1') \tan (\psi_1 + \mu) \tag{67}$$

$$\xi - \xi_1 + A_1 (\psi - \psi_1) = A_3 (x' - x_1'). \tag{68}$$

Substituting for ξ from equation (12) and solving for σ^* from the resulting expression, gives

$$\sigma^* = \exp \left\{ \frac{2}{\cot \phi} [\xi_1 - A_1 (\psi - \psi_1) - \psi + A_3 (x' - x_1')] . \right\} \tag{69}$$

Substitution for σ^* from equation (69) into equation (62) yields a transcendental equation in ψ and by solving this equation using an iteration technique, ψ is determined. x' and z' are determined as follows:

Along the wall

$$z' = - x' \tan (90 - \theta_0) \tag{70}$$

and therefore from equations (67) and (70)

$$x' = \frac{z_1' - x_1' \tan (\psi_1 + \mu)}{- \tan (90° - \theta_0) - \tan (\psi_1 - \mu)} . \tag{71}$$

From the values of σ^* and ψ determined for several points on the wall, $\sigma_n + H$ may be found from equation (48). The following expression is obtained for σ^* along the boundary of the active Rankine zone:

$$\sigma^* = \frac{\frac{\gamma l}{c_{vs}} z' + P}{1 + \sin \phi} + \beta_c z' \frac{\cot \phi}{1 + \sin \phi} \tag{72}$$

in which,

$$P = \frac{q}{c_{vs}} + \cot \phi .$$

In order that zones I and II (Fig. 4) do not overlap, the limiting values of θ_0 in the passive and active cases are as follows:

In the passive case

$$\theta_{0\,(cr)} = \frac{\triangle + \delta}{2} \tag{73}$$

and in the active case

$$\theta_{0\,(cr)} = \frac{\triangle - \delta}{2} \tag{74}$$

in which

$$\triangle = \sin^{-1}\left(\frac{\sin \delta}{\sin \phi}\right).$$

When δ is zero, $\theta_{0\,(cr)}$ is equal to zero in both the cases and when δ is equal to ϕ, $\theta_{0\,(cr)} = \pi/4 + \phi/2$ in the passive case and is equal to $\pi/4 - \phi/2$ in the active case.

Results and Discussion

Passive Earth Pressure

Numerical results are obtained for ϕ ranging from 0° to 40° and $\delta = 0$, $\phi/2$ and ϕ. In all the cases the value of x_M (Fig. 2 *a*) is assumed as 30 and is divided into 10 parts. Hence, the resultant pressure is determined at 11 points on the wall. The resultant pressure at the topmost point is denoted as p'_{0p} and that at the lowest point on the wall by p'_{np}. From the results obtained it is observed that the resultant pressure distribution along the wall is fairly linear and tends to a straight line asymptote as L increases as shown in Figs. 6 and 7 for the passive and active conditions respectively. Hence, the total pressure on the wall can be calculated without serious error by using the values of p'_{0p} and the slope of the asymptote. The slope of the asymptote is practically same as the slope of the secant between the last two points of the p_p' *versus* L curve. The modified coefficient of passive earth pressure is therefore given by

$$K_{pm} = \frac{p'_{np} - p'_{(n-1)p}}{L_n - L_{n-1}} \tag{75}$$

in which n stands for the total number of points on the wall. The total non-dimensional passive pressure acting on the wall may then be calculated using the following equation:

$$P_p = p'_{0p} L_n + \tfrac{1}{2} K_{pm} L_n^2 \tag{76}$$

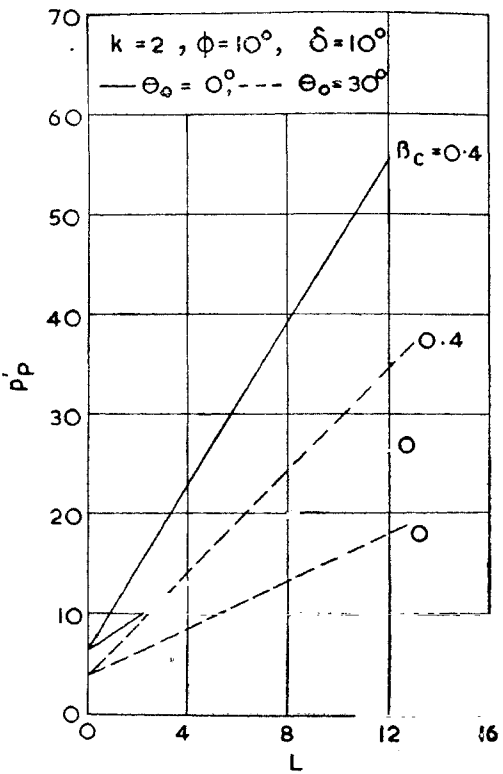

FIG. 6. Variation of resultant passive pressure along the wall.

Figures 8 *a* and 8 *b* are plotted for $\phi = 0°$ and 40°, respectively, in order to show the influence of k on p'_{γ}, for vertical wall and a wall inclined at $-30°$ with the vertical. It is found that when k changes from 0·8 to 2·0, p'_{γ} decreases by about 50 per cent.

In order to show the influence of k on the values of K_{pm}, Figs. 9 *a* and 9 *b* are plotted for $\phi = 0°$ and 40°, respectively, and $\theta_0 = 0°$ and $-30°$.

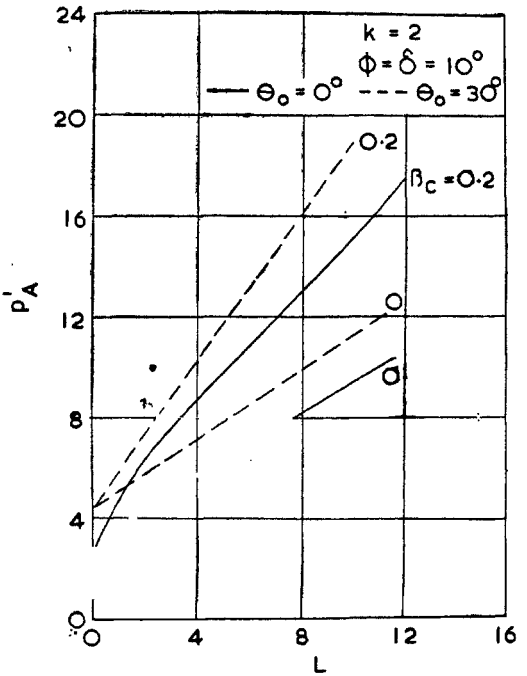

FIG. 7. Variation of resultant active pressure along the wall.

It is observed from these figures that the values of K_{pm} are considerably influenced by k when $\beta_c = 0{\cdot}4$ and are practically independent of k when $\beta_c = 0$. For $\beta_c = 0{\cdot}4$, it is found that when k changes from $0{\cdot}8$ to $2{\cdot}0$, K_{pm} decreases by about 30 per cent for $\phi = 0°$ and by about 20 per cent for $\phi = 40°$. Incidentally, Figs. 9 *a* and 9 *b* also show the considerable influence of θ_0 on K_{pm}.

The influence of β_c on K_{pm} is shown in Figs. 10 *a* and 10 *b* for $\phi = 0°$ and 40° respectively, and for $\theta_0 = 0°$ and $-30°$. It is observed that the values of K_{pm} are considerably affected by β_c. When β_c changes from 0 to $0{\cdot}4$, K_{pm} increases by about 130 per cent for $\phi = 0°$ and $k = 0{\cdot}8$,

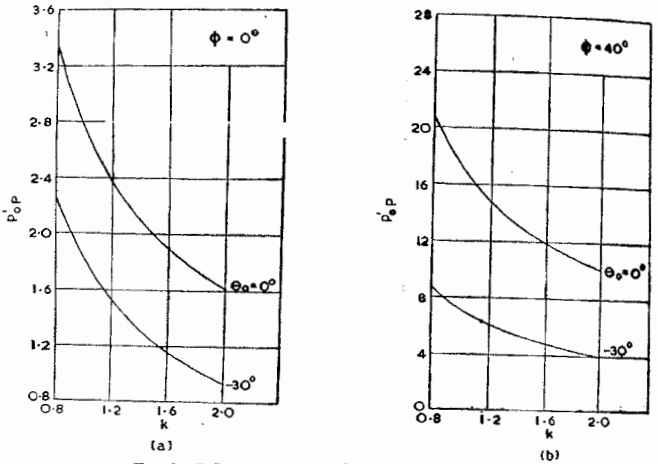

FIG. 8. Influence of k on p'_{0p}: (*a*) $\phi = 0°$ (*b*) $\phi = 40°$.

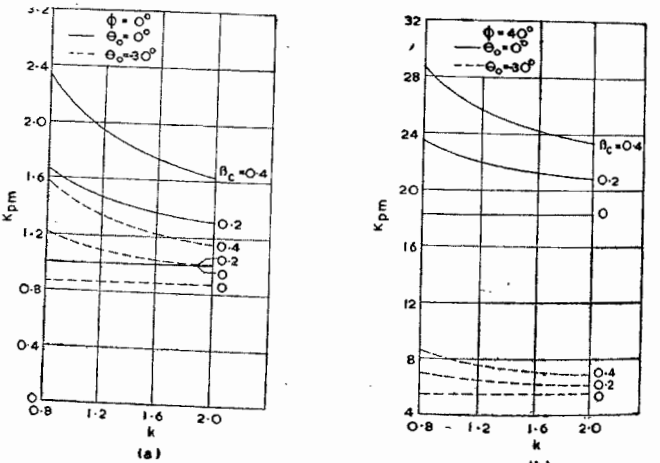

FIG. 9. Influence of k on K_{pm}: (*a*) $\phi = 0°$ (*b*) $\phi = 40°$.

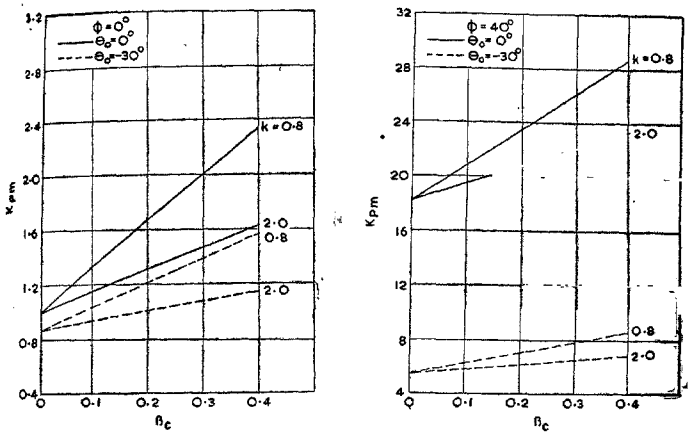

FIG. 10. Influence of β_c on K_{pm}: (*a*) $\phi = 0°$ (*b*) $\phi = 40°$.

whereas it increases by about 62 per cent for $\phi = 0°$ and $k = 2$. In the case of $\phi = 40°$, K_{pm} increases by about 58 per cent for $k = 0{\cdot}8$ and by about 20 per cent for $k = 2$.

Active Earth Pressure

In this case numerical results are obtained for ϕ ranging from 10° to 40°. The values of k and δ are the same as those in the previous case, whereas θ_0 is varied between 0° and $\theta_{0\,(cr)}$. The results are obtained for three values of β_c, *viz.*, 0, 0·1 and 0·2. Values of x_H (Fig. 4) are assumed as 6·0 and 4·2, respectively, for $\phi = 10°$, and 40°. The number of divisions into which x_H is divided for each of the above ϕ values is respectively, 21 and 15. Thus the resultant pressure, p_A' is obtained for several points along the wall. The resultant non-dimensional pressure at the topmost point on the wall is denoted by p'_{0A} and that at the lowest point on the wall by p'_{nA}. The modified active earth pressure coefficient, K_{Am}, is given by

$$K_{Am} = \frac{p'_{nA} - p'_{(n-1)A}}{L_n - L_{n-1}} \qquad (77)$$

in which $p'_{(n-1)A}$ = the resultant pressure at the point next to the lowest point on the wall.

The total active earth pressure acting on the wall is then calculated using the equation

$$P_A = p'_{oA} L_n + \tfrac{1}{2} K_{Am} L_n^2 \tag{78}$$

In order to show the influence of k on p'_{oA}, values of p'_{oA} for the extreme values of ϕ and for different values of θ_0, are plotted against k in Figs. 11 *a* and 11 *b*. It is observed that k has the maximum influence on

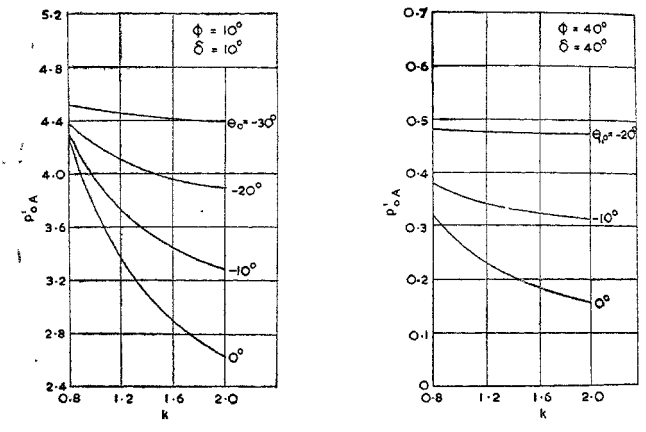

FIG. 11. Influence of k on p'_{oA}: (*a*) $\phi = 10°$ (*b*) $\phi = 40°$.

p'_{iA} when $\theta_0 = 0°$. Figures 12 *a* and 12 *b* show the influence of k on K_{Am} for extreme values of ϕ and β_c and $\theta_0 = 0°$ and $-20°$. It is observed from these figures that there is practically no influence of k on K_{Am} when $\beta_c = 0$. When $\beta_c = 0{\cdot}2$, it is observed that the influence of k is larger for $\theta_0 = 0$ compared to that for $\theta_0 = -20°$. Figures 13 *a* and 13 *b* show the influence of β_c on K_{Am} for the extreme values of ϕ and k, and $\theta_0 = 0°$ and $-20°$. It is observed from these figures that K_{Am} varies almost linearly with β_c, and it has a greater influence for $k = 0{\cdot}8$ when compared to that for $k = 2{\cdot}0$.

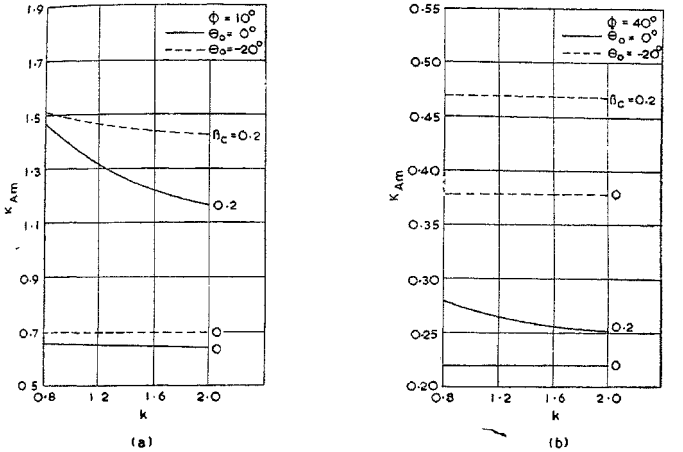

FIG. 12. Influence of k on K_{Am}: (*a*) $\phi = 10°$ (*b*) $\phi = 40°$.

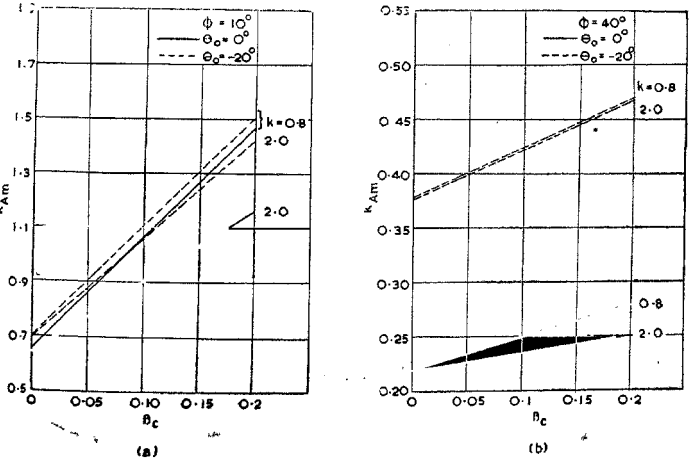

FIG. 13. Influence of β_c on K_{Am}: (*a*) $\phi = 10°$ (*b*) $\phi = 40°$.

The influence of k as well as that of δ on the $(\psi + \mu)$-slip lines is shown in Fig. 14 *a* for $\phi = 10°$ and $\beta_c = 0$. It is observed from this figure that for the same depth of wall, the rupture surface for $k = 2$ is below that for $k = 1$. However, the effect of k is small. When δ changes from 5° to 10°, it is observed that the rupture surface becomes deeper and more curved. Figs. 14 *b* shows the influence of β_c on the $(\psi + \mu)$-slip lines for $\phi = 10°$ and $k = 1$. It is observed from this figure that for the same depth of wall the rupture surface for $\beta_c = 0{\cdot}4$ is shallower than that for $\beta_c = 0$.

To show the utility of the results presented and for comparison of the results with those of the conventional methods, an example is worked out below.

Example.—Find the resultant force on the retaining wall for the passive case for the following data.

Height, H, of the retaining wall = 5 m,

$$\theta_0 = 0, \gamma = 2{\cdot}0 \text{ g/cc}, \qquad c_v = 0{\cdot}2 \text{ kg/cm}^2, \qquad \beta_c = 0$$

and

Case 1: $\phi = 0, \quad k = 2$

Case 2: $\phi = 0, \quad k = 1$

Case 3: $\phi = 0, \quad k = 0{\cdot}8$.

Ans.: Case 1: From Figs. 8 *a* and 9 *a*, for

$\phi = 0, \quad \beta_c = 0, \quad \theta_0 = 0$ and $k = 2, \quad p'_{\sigma p} = 1{\cdot}61$ and

$K_{pm} = 1{\cdot}0$

$$l = \frac{c_v}{\gamma} = \frac{200}{2} = 100 \text{ cm}$$

$$L = \frac{500}{100} = 5$$

$$P_p = [p'_{\sigma p} L_n + \tfrac{1}{2} K_{pm} L_n^2] \gamma l^2$$

$$= [1{\cdot}61 \times 5{\cdot}0 + \tfrac{1}{2} \times 1 \times 5 \times 5] 2{\cdot}0 \times 100 \times 100 \text{ g/cm}$$

$$= 4{\cdot}11 \times 10^5 \text{ g/cm}$$

$$= 41{\cdot}1 \text{ tonnes/m}$$

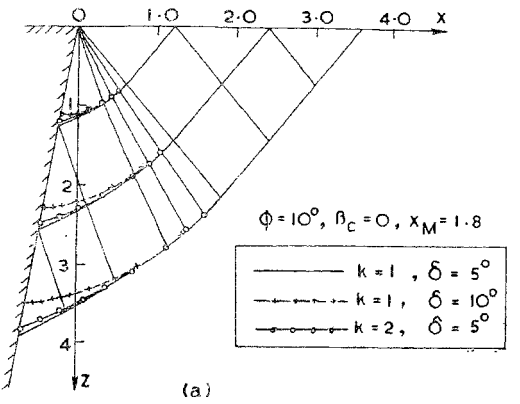

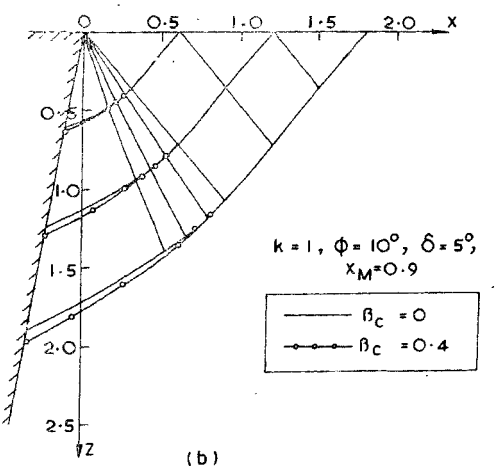

FIG. 14. Influence of: (*a*) k and δ (*b*) β_a, on the rupture surface in the active case.

Case 2: From Figs. 8 *a* and 9 *a* for $\phi = 0$,

$$\beta_c = 0,\ \theta_0 = 0 \quad \text{and} \quad k = 1. \quad p'_{ep} = 2{\cdot}75 \quad \text{and} \quad K_{pm} = 1{\cdot}0$$

$$P_p = [2{\cdot}75 \times 5{\cdot}0 + \tfrac{1}{2} \times 1{\cdot}0 \times 5 \times 5]\ 2 \times 100 \times 100 \text{ g/cm}$$

$$= 52{\cdot}5 \text{ tonnes/m.}$$

Case 3: From Figs. 8 *a* and 9 *a* for this case

$$p'_{ep} = 3{\cdot}34 \quad \text{and} \quad K_{pm} = 1{\cdot}0$$

$$P_p = [3{\cdot}34 \times 5 + \tfrac{1}{2} \times 1{\cdot}0 \times 5 \times 5]\ 2 \times 100 \times 100 \text{ g/cm}$$

$$= 58{\cdot}4 \text{ tonnes/m.}$$

Using Rankine's approach

$$P_p = 2cH + \frac{\gamma H^2}{2}$$

$$= 2 \times 200 \times 500 + 2 \times \frac{500 \times 500}{2} \text{ g/cm}$$

$$= 45 \text{ tonnes/m.}$$

It is seen from the example that the resultant force for the present example varies from 41·1 to 58·4 tonnes/m as k varies from 2 to 0·8 whereas Rankine's theory gives a value of 45 tonnes/m. From the example it is apparent that the influence of anisotropy is considerable and it should not be neglected.

CONCLUSIONS

The influence of k and β_c on the resultant pressures, p'_{0p} and p'_{0A} and on the coefficients K_{pm} and K_{Am}, are studied herein. The results show that as k changes from 0·8 to 2·0, p'_{0p} and p'_{0A} decrease considerably for small inclinations of the wall with the vertical. Further it is found, that K_{pm} as well as K_{Am} are more influenced by k for higher values of β_c and are practically unaffected by k when $\beta_c = 0$. The influence of β_c on K_{pm} and K_{Am} is greater than that of k and is higher for smaller values of k. The results have also shown clearly that the variation of the resultant pressure along the wall is almost linear for both the passive and active cases. Hence, the total earth pressure in either case can be determined with sufficient accuracy by knowing the resultant pressure at the topmost point of the wall and the slope of the asymptote to the resultant pressure curve.

REFERENCES

[1] Sokolovsky, V. V. .. *Statics of Granular Media*, Pergamon Press, London, 1965.

[2] Wack, B. .. Etude de la Butee d'un Ecran Plan Contre un Massif Coherent par la Theorie des Caracteristiques, *Doctoral Thesis*, University of Grenoble, France, 1960.

[3] Hajal, M. .. Etude General de la Butee d'un Ecran Plan Contre un Massif Coherent par la Theorie des Caracterisques, *Doctoral Thesis*, University of Grenoble, France, 1961.

[4] Livneh, M. and Shklarsky, E. The Bearing capacity of asphaltic concrete carpets suracing, Proceedings, International Conference on the Structural Design of Asphalt Pavements. *Ann. Arbour, Michigan*, 1962, pp. 345–353.

[5] Casagrande, A. and Carrillo, N. *Shear Failure of Anisotropic Materials.* Journal of the Boston Society of Civil Engineers, Reprinted in Contributions to Soil Mechanics, 1941–1953, pp. 122–135.

[6] Shklarsky, E. and Livneh, M. *Equation of Slip Lines in an Anisotropic-Cohesion Medium.* Bulletin of the Research Council of Israel, 1962, **10 C**, pp. 159–170.

[7] Siva Reddy, A. and Srinivasan, R. I. *Bearing Capacity of Footings on Anisotropic Soils.* Journal of the Soil Mechanics and Foundations Division, ASCE, 1970, 96, pp. 1967–1986.